EurJOC
European Journal of Organic Chemistry

Highly Conjugated Systems

E. Arias, I. Moggio,* R. Torres,
R. F. Ziolo, J.-L. Maldonado, K. Green,
T. M. Cooper, G. Wicks, A. Rebane,
M. Drobizhev, N. S. Makarov,
M. Ottonelli, G. Dellepiane 1–13

Direct Synthesis of 2,5-Bis(dodecanoxy)-phenyleneethynylene-Butadiynes by Sonogashira Coupling Reaction

Keywords: Alkynes / Conjugation / Chain structures / Nonlinear optics / UV/Vis spectroscopy

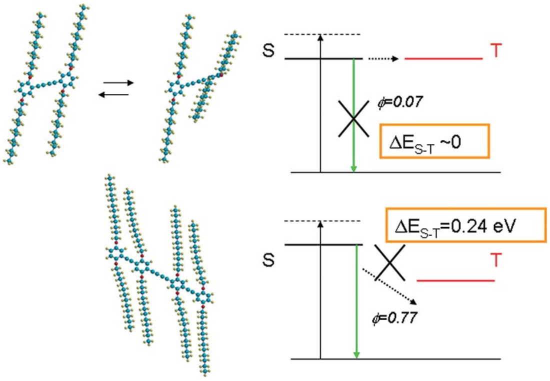

An alternative strategy that can be used to obtain phenyleneethynylene-butadiynes through Sonogashira reaction is reported. A combined spectroscopic and theoretical study reveals that the dimer behaves like a diacetylene, whereas the longer oligomers present large quantum yield due to larger energy gaps between the singlet and triplet excited states.

DOI: 10.1002/ejoc.201300230

Direct Synthesis of 2,5-Bis(dodecanoxy)phenyleneethynylene-Butadiynes by Sonogashira Coupling Reaction

Eduardo Arias,[a] Ivana Moggio,*[a] Román Torres,[a] Ronald F. Ziolo,[a] José-Luis Maldonado,[b] Kirk Green,[c] Thomas M. Cooper,[d] Geoffrey Wicks,[e] Aleksander Rebane,[e] Mikhail Drobizhev,[e] Nikolay S. Makarov,[e] Massimo Ottonelli,[f] and Giovanna Dellepiane[f]

Keywords: Alkynes / Conjugation / Chain structures / Nonlinear optics / UV/Vis spectroscopy

The synthesis of a 2,5-bis(dodecanoxy)phenyleneethynylene-butadiyne series with 2, 4, 6 and 8 phenyl rings is reported. Sonogashira coupling reaction, rather than the Glaser/Eglinton/Hay reactions classically used for butadiyne formation was applied. The molecular structures of all compounds were confirmed by ^{1}H, DEPT-135, APT ^{13}C, MALDI-TOF, FTIR and FT-Raman analyses. The linear and nonlinear optical properties were studied in solution by UV/Vis, static and time-resolved fluorescence, and by two-photon absorption (2PA) spectroscopy. With the exception of the dimer, for which intersystem crossing is very favoured due to the low energy gap between the singlet and triplet states as theoretically predicted, the other oligomers present high fluorescence quantum yields (0.77–0.82) and large cross-sections (up to 5000 GM for the octamer) that could be applied in multiphoton microscopy or nonlinear optics.

Introduction

Because phenyleneethynylene (PE) oligomers have potential applications in optoelectronics, new synthetic routes have been explored to generate such compounds in fewer steps and in higher yields; the routes are designed to encompass all types of molecular architecture such as linear, cross, stars, hyperbranched, or dendritic types to obtain a specific supramolecular order.[1] The Sonogashira reaction is a well-known cross-coupling reaction that takes place with an acetylene and a bromo or iodoaryl through the catalytic action of a Pd^0/CuI complex, whereby a small amount of diacetylene as byproduct is always formed. Because the catalytic complex is rich in electrons, the substituents in the aryl groups have an important effect on the reaction yield; electron-withdrawing rather than -donating groups favour the cross-coupling, however, even when yields of the desired product are always higher than 50 %, usually the amount of diacetylene formed as byproduct is not reported. Butadiynes can also be formed in poly(phenylenethynylene) compounds and are usually considered as structural defects because they can polymerize in the solid state, giving cross-linked insoluble materials.[2] Nevertheless, oligo(*p*-phenylenebutadiynylene) and oligo(phenyleneethynylene-butadiyne) compounds have been reported as defined molecular rods and interesting self-assembling properties have been reported.[3] Diacetylenes are usually prepared by Cadiot–Chodkiewicz coupling reaction for asymmetrical butadiynes or oxidative dimerization of a terminal acetylene for symmetric diacetylenes by either Glaser, Eglinton or Hay reactions; details on these reactions are reported in a recent review by Diederich et al.[4] With the aim of providing novel materials with balanced hole and electron transport properties, Klemm et al. reported in 2002 the synthesis of highly luminescent hybrid phenyleneethynylene-phenylenevinylene copolymers.[5] As part of the strategy, they synthesized a central trimer by the Sonogashira cross-coupling reaction between 1,4-diethynyl-2,5-bis(2-ethylhexyloxy)benzene and 4-bromobenzaldehyde, however, in addition to the desired product, they also isolated the 1,4-bis{4-formylphenylethynyl-[2,5-bis(octadecyloxy)phenyl]buta-1,3-diyne} compound as a byproduct of the reaction, suggesting that self-coupling of acetylenes of alkoxy phenyls gives rise to the formation of butadiynes and, in particular, phenylene-

---

[a] Centro de Investigación en Química Aplicada,
Boulevard Enrique Reyna 140, 25294 Saltillo, Mexico
Fax: +52-844-4389839
E-mail: ivana.moggio@ciqa.edu.mx
Homepage: www.ciqa.mx
[b] Centro de Investigaciones en Óptica,
Loma del Bosque 115, Col. Lomas del Campestre, 37150 León, México
[c] Department of Chemistry, McMaster University,
1280 Main St. W, Hamilton, Ontario, L8S 4M1, Canada
[d] Materials and Manufacturing Directorate, Air Force Research Laboratory,
3005 Hobson Way, Wright-Patterson Air Force Base, Ohio 45433, USA
[e] Physics Department, Montana State University,
Bozeman, Montana 59717, USA
[f] Dipartimento di Chimica e Chimica Industriale, Universitá di Genova,
Via Dodecaneso 31, Genoa 16146, Italy

Supporting information for this article is available on the WWW under http://dx.doi.org/10.1002/ejoc.201300230.

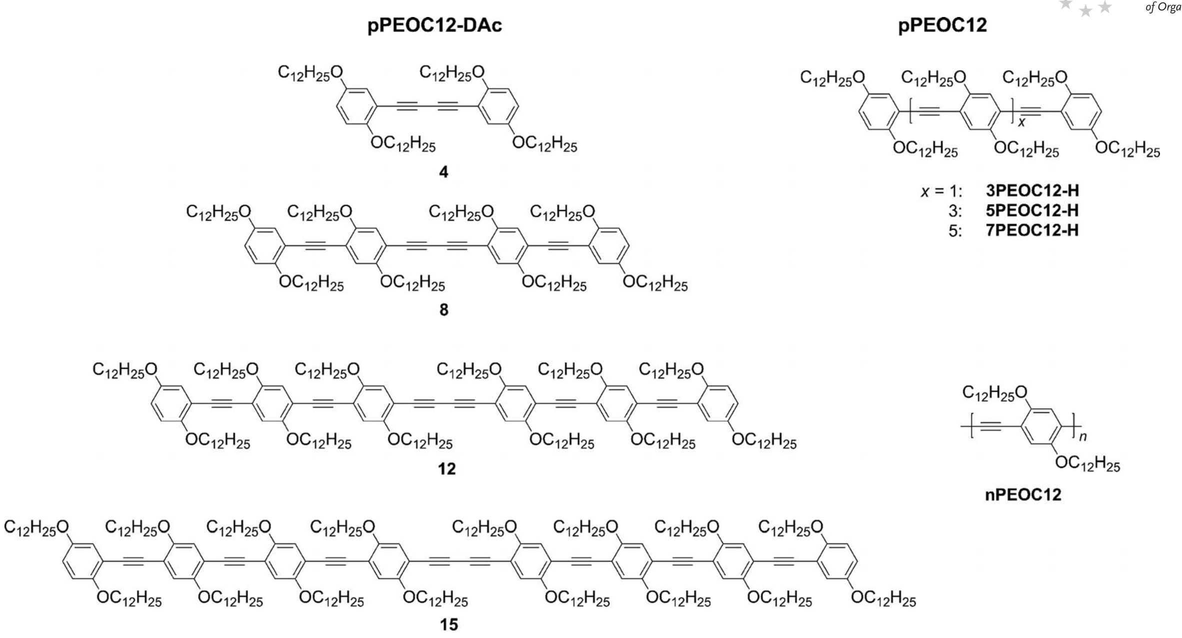

Figure 1. Chemical structure of (left side) 2,5-bis(dodecanoxy)phenyleneethynylene-butadiyne (pPEOC12-Dac) series of this work: dimer **4**, tetramer **8**, hexamer **12** and octamer **15** as per Scheme 1. (Right side) 2,5-bis(dodecanoxy)phenyleneethynylene (pPEOC12) series studied in ref.[8] and here used as term of comparison for the discussion of the optical properties.

ethynylene-butadiyne structures are feasible by the Sonogashira reaction. For this oligomer, the authors demonstrated that the diyne segment confers a stronger transition moment, which results in a higher absorption coefficient and enhanced radiative rate constant. The major part of the work was devoted to a comparison of the electrochemical, photophysical and photoconductivity properties of the resultant copolymers and concluded that the diyne-containing polymers present higher photoconductivity and stability, stronger electron-accepting properties and higher quantum yields in the solid state. Other alkoxy-substituted phenyleneethynylenes bearing central butadiynes were also synthesized by Thomas' group by combining the Glaser oxidative reaction with the Sonogashira reaction. They demonstrated by STM that these materials exhibit a very particular supramolecular arrangement when deposited on HOPG.[3c]

In the present work, we report the synthesis of a series of phenyleneethynylene-butadiynes (pPEOC12-Dac, Figure 1) for which the length of the phenyleneethynyene segment increases from 1 to 4. Hereafter, these compounds will be referred to as dimer, tetramer, hexamer or octamer on the basis of the total number of phenyl rings. The phenyleneethynylene-butadiynes were prepared in high yield by the Sonogashira coupling reaction. In particular, we found that as the electron-donating character of the 2,5-bis(dodecanoxy)phenyleneethynylene-acetylene-terminated oligomer increases by extension of the number of repetitive units, its cross-coupling with the halogen-aryl decreases, leading to the formation of the diacetylene oligomer as the main product. In this way, for instance, the Pd^0/CuI cross-coupling of an acetylene terminated tetramer with iodo-2,5-bis(dodecanoxy)benzene yields the expected pentamer in only ca. 3%, whereas the diacetylene octamer was obtained in 89% yield. A physicochemical study by combining different spectroscopic techniques (NMR, UV, fluorescence and Raman) with theoretical simulations on the dimer and tetramer was also carried out in an attempt to explain the different photophysical properties of the dimer with respect to the longer oligomers. Quite large two-photon cross-sections (up to 5000 GM for the octamer) were found that could be applied in multiphoton microscopy or nonlinear optics.

Results and Discussion

Synthesis and Molecular Structure Characterization

The pathway used to synthesize the pPEOC12-Dac series is depicted in Scheme 1. The convergent synthesis, in general, involves only two repetitive reactions: a Pd/Cu cross-coupling reaction and desilylation of the protected acetylene groups.[6] In particular, the Pd/Cu cross-coupling reactions were carried out by adapting the Godt protocol, whereby aryliodides are coupled to acetylenes at 0 °C, whereas for aryl bromides the solvent was heated to reflux at ca. 80 °C.[7]

The oligomerization starts with the Pd/Cu cross-coupling of one equivalent of **1** and **2** to generate the bromine-terminated dimer **3** in 64% yield. From this reaction, the diacetylene dimer **4** was isolated in 30% yield. We observed that in all reactions for which the oligomers were acetylene-terminated and a Pd/Cu cross-coupling reaction was involved, the diacetylene was always isolated as a byproduct in large amounts. From this observation, we conducted an exploratory reaction by adding the acetylene-terminated monomer **1** and the catalyst complex in a typical molar

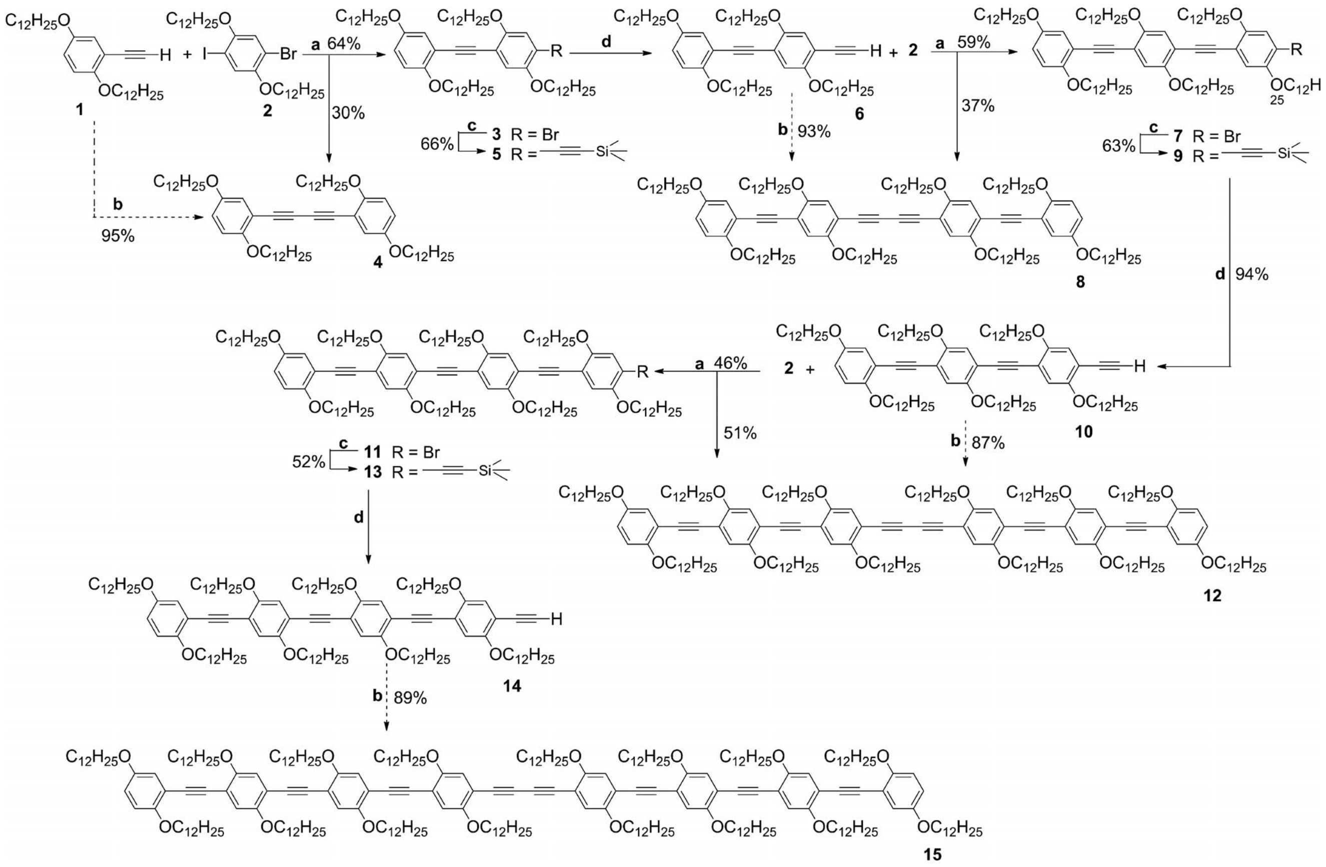

Scheme 1. Synthetic route for the pPEOC12-Dac series. *Reagents and conditions:* (a) [$(Ph_3P)_2PdCl_2$] (2.5 mol-%), CuI (1.5 mol-%), NEt_3, THF, 0 °C; (b) [$(Ph_3P)_2PdCl_2$] (2.5 mol-%), CuI (3.0 mol-%), NEt_3, THF, 80 °C; (c) [$(Ph_3P)_2PdCl_2$] (2.5 mol-%), CuI (1.5 mol-%), TMSA, NEt_3, THF, 60 °C; (d) TBAF, THF, room temp.

ratio of [$[(C_6H_5)_3P]_2PdCl_2$] (2.5 mol-%)/CuI (1.5 mol-%) in degassed Et_3N, and obtained the diacetylene dimer **4** as the main product in 95% yield. A similar result was obtained in the absence of CuI, although longer reaction times were necessary. No differences were observed by changing the palladium catalyst molar ratio or when the amount of CuI was increased to 3.0 mol-%; the self-coupling acetylene–acetylene proceeded to completion in two hours. From these results, for further reactions, 2 mol-% CuI was used, depending on the coupling type reaction; for instance, to favour the coupling between an acetylene and a bromoaryl (ca. 80 °C) or iodoaryl (ca. 0 °C), a 1.5% molar ratio of CuI was determined to be suitable, whereas for acetylene–acetylene coupling reactions the use of 3.0 mol-% CuI provided quantitative yields when the palladium complex was kept at a 2.5% molar ratio. Bromine-terminated dimer **3** was subjected to Pd/Cu cross-coupling reaction with TMSA to afford dimer **5** in 66% yield. Desilylation of **5** gave acetylene-terminated dimer **6**, which was subjected to Pd/Cu mediated cross-coupling with one equivalent of **2** at 0 °C to generate bromine-terminated trimer **7** in 59% yield; the diacetylene tetramer **8** was also recovered as a byproduct in 37% yield. Acetylene-terminated dimer **6** was acetylene-acetylene coupled to form diacetylene tetramer **8** in 93% yield. Subsequently, bromine-terminated trimer **7** was subjected to another cycle of Pd/CuI coupling with TMSA to afford **9** in 63% yield, which, after desilylation, gave acetylene-terminated trimer **10**. One equivalent of **10** then underwent Pd/CuI mediated cross-coupling to generate bromine-terminated tetramer **11** (46% yield) and diacetylene hexamer **12** (51% yield) as a byproduct. The self-coupling of **10** afforded hexamer **12** in 87% yield. Finally, bromine-terminated tetramer **11** was subjected to another TMSA cross-coupling-desilylation cycle to form the acetylene-terminated tetramer **14**, from which, after acetylene-acetylene Pd/Cu coupling, octamer **15** was obtained in 89% yield.

^1H and ^{13}C, DEPT-135 and APT ^{13}C NMR spectroscopy were essential to corroborate the molecular structures of the oligomers. Figure 2 (a) collects the ^1H NMR spectra of the series with two expanded regions in Figure 2 (b and c). Figure 2 (d) shows the ^{13}C NMR spectrum of tetramer **8** with the corresponding notations in the inserted chemical structure, as an example. In Figure 2 (a), two different aromatic proton signals are identified in the series: those in the *ortho* position with respect to the triple bonds ($H_{o\text{-ynes}}$), and four protons that are *meta* and *para* to the triple bonds. The latter four protons are positioned with two at each of the phenyl rings at the extremity of the oligomers and are labelled as H_{ext}. In the aliphatic region at ca. 4.0 ppm, two triplets appear corresponding to the protons α to the oxygen of the two dodecanoxy chains, which are different one to the other; one set being the $-CH_2-$ in the δ position to

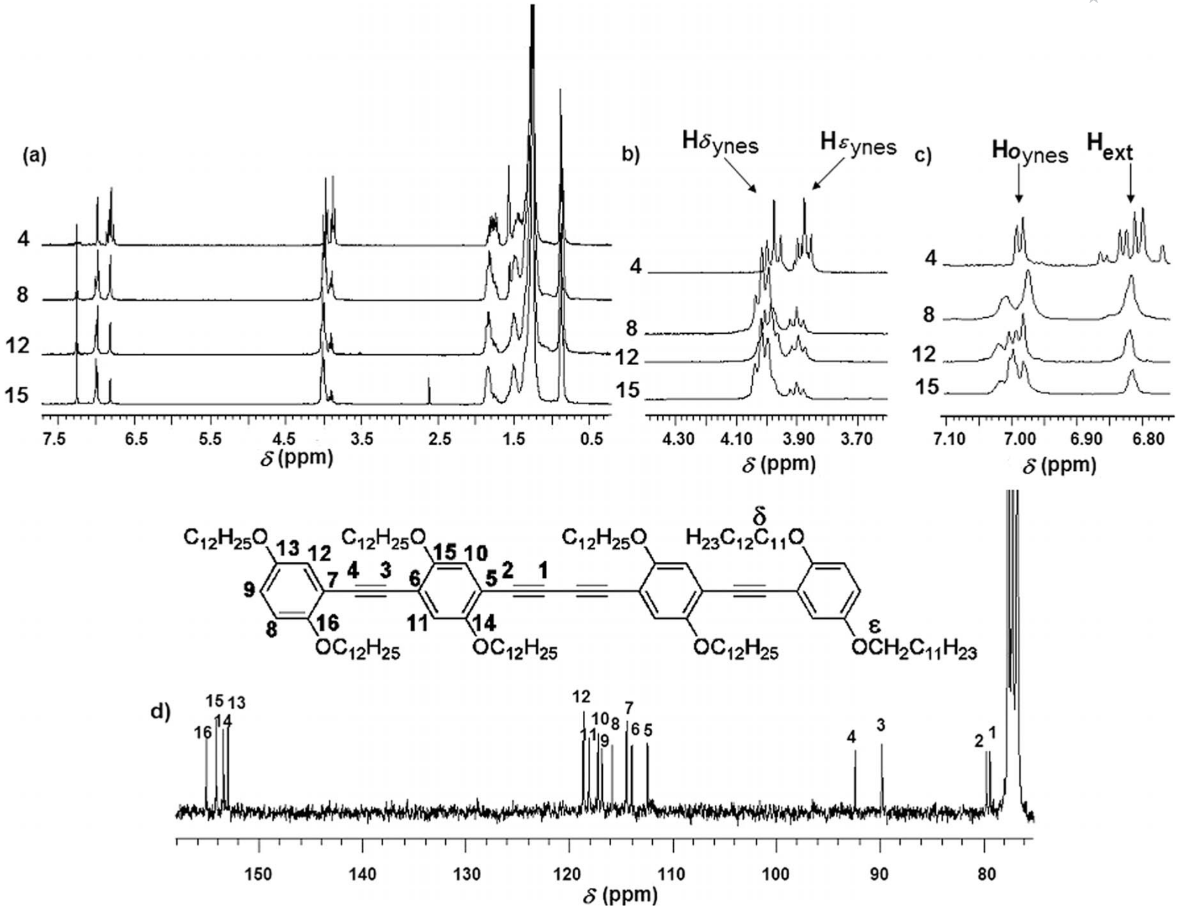

Figure 2. NMR spectra in $CDCl_3$: (a) ^1H (300 MHz) of the pPEOC12-Dac series; (b) expansion of the corresponding aliphatic –O–CH_2- and (c) aromatic region, and (d) the conjugated region of the ^{13}C NMR spectrum (75 MHz) of tetramer **8** with the corresponding annotations on the chemical structure for assignment.

triple bonds ($H_{\delta\text{-ynes}}$) centred at 4.0 ppm, whereas those in the ε position to the triple bonds ($H_{\varepsilon\text{-ynes}}$) appear at δ = 3.89 ppm, Figure 2 (b). As the oligomer length increased, the integration of the $H_{\delta\text{-ynes}}$ also increased because of the large number of –CH_2– groups. A similar behaviour was also observed in the aromatic region (Figure 2, c); the intensity of the $H_{o\text{-ynes}}$ increases with oligomer length whereas the intensity of the H_{ext} signal remained constant. The theoretical factor for the integration ratio between the $H_{\delta\text{-ynes}}$ and the total number of aromatic protons gives: 1.33, 1.6, 1.71, 1.78 for dimer **4**, tetramer **8**, hexamer **12** and octamer **15**, respectively, whereas the experimental values were 1.34, 1.74, 1.8 and 1.91. In the same way, the theoretical factor of integration ratio between $H_{o\text{-ynes}}/H_{ext}$ gives 0.5, 1.5, 2.5 and 3.5, which are values that match better with the observed values of 0.45, 1.7, 2.6 and 3.7, respectively, for the series. These factors are more useful indicators of oligomer structure than the integration itself because the number of protons obtained by integrating each individual peak does not match well with the expected structure as the oligomer length is increased, particularly those corresponding to the aliphatic chains.

We believe that this behaviour could be due to the fact that even in solution (most of these compounds require warming to completely dissolve), the oligomers have strong intermolecular interactions that favour agglomeration. We confirmed this hypothesis when, after a few days at room temperature, a cotton-like precipitate was formed from a concentrated chloroform solution, which, in turn, could be redissolved upon gentle heating. However, despite this behaviour, attempts to grow single crystals failed.

In the ^{13}C NMR spectra (illustrated in Figure 2 (d) for tetramer **8**), two different acetylene carbon resonances were clearly identified: the diacetylene signals that appear at ca. 79.1–79.9 ppm and the ethynes/phenyl signals that give signals centred at 88.9–92.5 ppm. It can be seen that all aromatic and ethyne carbon resonances are chemically distinct, including those of the ether substituted ring that appear as four peaks at 150.3–155.2 ppm. The remaining eight aromatic carbon signals are centred at 114.0–118.77 ppm. A similar behaviour is observed for hexamer **12**, for which two acetylene, two ethyne, six signals for the aromatic carbon atoms substituted with ethers, and twelve signals for the rest of the aromatic carbon atoms are clearly identified. In the spectrum of octamer **15** some signals overlap. The COSY and HETCOR spectra confirm that all hydrogen–hydrogen and carbon–hydrogen correlations match well with the corresponding structures.

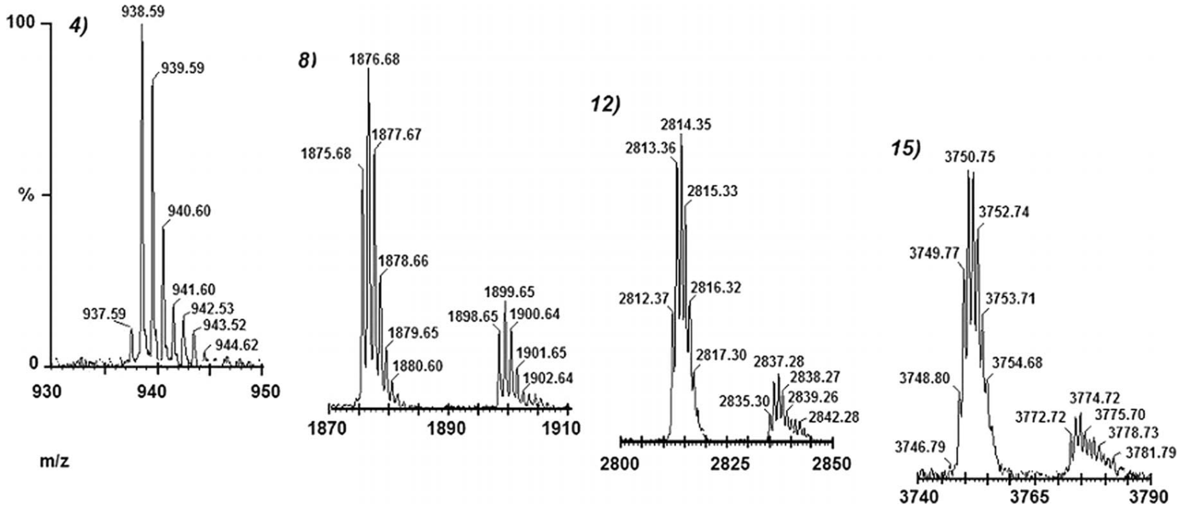

Figure 3. MALDI-TOF MS (region of the molecular ion peak) for the pPEOC12-Dac series.

Positive Matrix-Assisted Laser Desorption Ionization Time-of-Flight Mass Spectrometry (MALDI-TOF-MS) analysis supported the molecular structure of the oligomers by showing their expected molecular ion peak (Figure 3); For **4**: *m*/*z* 938.6 (M^+, calcd. for $C_{64}H_{106}O_4$: 938.8), for **8**: *m*/*z* 1875.7 (M^+, calcd. for $C_{128}H_{210}O_8$: 1875.6), for **12**: *m*/*z* 2812.4 (M^+, calcd. for $C_{192}H_{314}O_{12}$: 2812.4), for **15**: *m*/*z* 3748.8 (M^+, calcd. for $C_{256}H_{418}O_{16}$: 3749.2). The isotopic resolution decreases along with the conjugation and its distribution pattern is consistent with the oligomer size, giving more peaks for the octamer as there are more isotopic carbon atoms present in the molecule. It should also be noted that the signals at higher molecular weight (molecular ion weight +22.99) are attributed to Na^+ cationization.[9]

Figure 4 shows the IR spectra for monomer **1** and octamer **15** as representative molecules of the pPEOC12-Dac family. The monomer **1** clearly shows the intense ≡C–H stretching band at 3286 cm^{-1} that, as expected, disappears for octamer **15** as well as for the rest of the series. The most interesting region is that related to the –C≡C– stretching band, which should give a very weak signal at around 2200 cm^{-1} for the acetylenic triple bonds vibration and no signal at all for the internal diacetylenic group, due to the symmetry of the molecules.[10] In contrast, both –C≡C– stretching bands are expected to give a very intense Raman signal at almost the same wavenumber. In agreement with this expectation, the IR spectrum presents a very weak signal at around 2200 cm^{-1}, whereas a very intense peak in the Raman spectra appears at 2200 ± 2 cm^{-1}. Dimer **4** represents an exception, with no bands in the IR whereas the Raman signal moves to 2220 cm^{-1}.

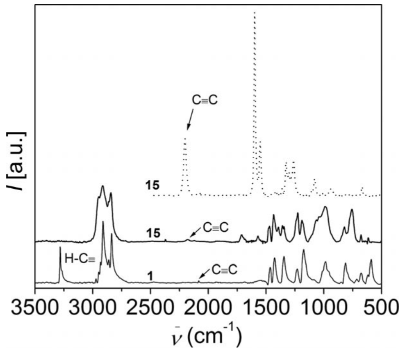

Figure 4. From bottom to top: infrared spectra (solid lines) of monomer **1** and octamer **15**, Raman spectrum (dotted line) of octamer **15**.

It should be noted that the oligomers do not exhibit topochemical polymerization[11] either by UV irradiation or thermally, and are stable at air and at room temperature for extended periods.

Optical Properties and Theoretical Calculations

Figure 5 shows the absorption and fluorescence spectra of the pPEOC12-Dac series in $CHCl_3$; the optical properties are presented in Table 1.

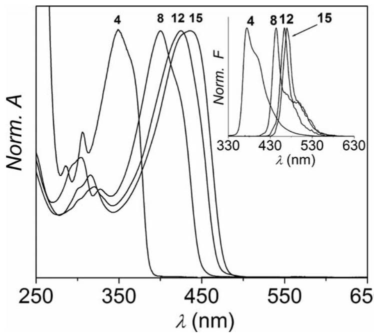

Figure 5. Absorption and fluorescence (insert) spectra in $CHCl_3$ for the pPEOC12-Dac series.

For comparison, relevant optical properties of 2,5-bis(dodecanoxy)phenyleneethynylenes (pPEOC12, chemical structure shown in Figure 1) are reported in this section. Details on the synthesis and spectroscopic properties of these molecules have been reported.[8] In general, the spectral features of pPEOC12-Dac are very similar to those pre-

Table 1. Optical properties of pPEOC12-Dac in $CHCl_3$.

pPEOC12-Dac	λ_{abs} [nm]	$HHBW_{abs}$ [nm][a]	$\varepsilon \times 10^4$ [$M^{-1}cm^{-1}$]	λ_{em} [nm]	Stokes' shift [cm^{-1}]	$HHBW_{fluo}$ [nm][a]	Φ_F[b]	τ [ns]	$k_F \times 10^9$ [s^{-1}]	$k_{nr} \times 10^9$ [s^{-1}]
Dimer **4**	350	64	1.68	387	2732	49	0.07	0.42 ± 0.2%	0.18	2.20
Tetramer **8**	400	68	7.39	444	2477	23	0.77	0.87 ± 0.2%	0.88	0.26
Hexamer **12**	425	74	11.60	463	1931	23	0.78	0.72 ± 0.3%	1.08	0.30
Octamer **15**	435	77	16.99	470	1712	24	0.82	0.69 ± 0.4%	1.19	0.26

[a] Half height band width. [b] ±10%.

viously reported for the pPEOC12. (1) The absorption spectra are very broad (half-height band width (HHBW) around 70 nm), whereas the fluorescence spectra are of the excitonic type with smaller HHBW because the planarization of the geometry in the excited state reduces the conformation distribution with respect to the ground state. The change in the geometry from ground to excited state is confirmed also for this series with the Stokes' shift ranging from the value of aromatic systems (around 1430 cm^{-1}) to those of biphenyls, which assume a more planar conformation after excitation (ca. 3310 cm^{-1}).[12] In this respect, dimer **4** has the higher value for the Stokes' shift. (2) The absorption spectra present an intense peak due to the HOMO–LUMO transition, which redshifts along with an increase in the oligomer length. The corresponding molar absorption coefficient ε increases in accordance with the higher chromophore content. Higher energy peaks can be observed in the 300–320 nm range and ascribed to electronic transitions from lower lying occupied orbitals.[13] (3) The absorption spectra do not change with concentration or solvent polarity, excluding the possibility of any ground-state interactions such as aggregation[13a] (see the Supporting Information). (4) The fluorescence spectra are independent of the excitation wavelength, and the excitation spectra are the same when the emission peak is fixed at the more intense peak or to the shoulder, confirming that only one emitting state exists (see the Supporting Information). It can be observed that dimer **4** absorbs at lower wavelength than dodecanoxy trimer 3PEOC12-H[8] (350 vs. 380 nm) and tetramer **8** absorbs at wavelengths between 3PEOC12-H and the dodecanoxy phenyleneethynylene pentamer 5PEOC12-H (412 nm),[8] in accordance with the level of conjugation. However, hexamer **12** and octamer **15** present absorption maxima at higher wavelength than heptamer 7PEOC12-H and even the pPEOC12 homopolymer and have higher molar absorption coefficient,[8] suggesting that the presence of the central diacetylene group increases the π-π overlap in the ground state with respect to the phenyleneethynylenes. Similar behaviour was found by Klemm et al. in a study that compared the optical properties of a phenyleneethynylene aldehyde tetramer with those of the corresponding diyne containing oligomer, i.e., the maximum absorption wavelength and relative molar absorption coefficient were higher for the diyne oligomer with respect to the phenyleneethynylene.[5] (5) Fluorescence quantum yields are very high for tetramer **8**, hexamer **12** and octamer **15**, and are in the same range as those reported for H-terminated phenyleneethynylenes.[8] In contrast, dimer **4** presents a very low quantum yield.

The fluorescence decays obtained by time-correlated single-photon counting (TCSPC) can be well-fitted with a monoexponential curve, supporting the conclusion that there is only one emitting state. Figure 6 illustrates the decay and fit for octamer **15** as an example, together with the weighted residuals. The TCSPC results for the other oligomers are reported in the Supporting Information.

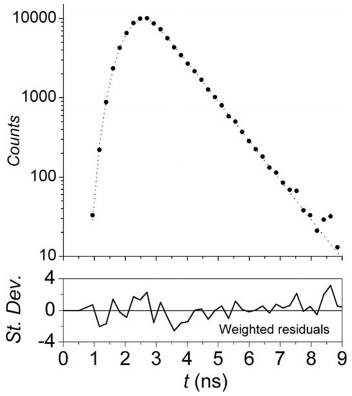

Figure 6. TCSPC data for tetramer **8** in chloroform.

The corresponding lifetimes are in the same range as those reported for alkoxy phenyleneethynylenes[14] and the diyne oligomer reported by Klemm.[5] The value decreases from tetramer **8** to octamer **15** along with an increase in the radiative rate constant K_f, in agreement with the higher extinction coefficient. The nonradiative constant K_{nr} is practically constant. A particular case is dimer **4**, for which the lifetime is lower, giving a K_{nr} much higher than the other oligomers. This suggests stronger nonradiative losses. As previously discussed, this oligomer presents a larger Stokes' shift, which implies higher internal conversion losses. However, the large decrease in the fluorescence quantum yield and large nonradiative constant could also be due to intersystem crossing to the triplet state, as reported for different types of diphenylpolyynes.[15]

To investigate the possibility of intersystem crossing, molecular mechanics theoretical simulations were performed on dimer **4** and tetramer **8**. Figures 7 and 8 report some representative conformers obtained within this study for the two oligomers. For dimer **4** (Figure 7), a negligible energy difference of about 0.3 kcal/mol is predicted between the conformers with the phenyl rings dihedral angles near 0° (D1) and 80° (D2), respectively. Nevertheless, the strong dependence of the relative conformational energy on the "randomization" of the aliphatic tails should be emphasized and this could be strongly correlated with the environment in

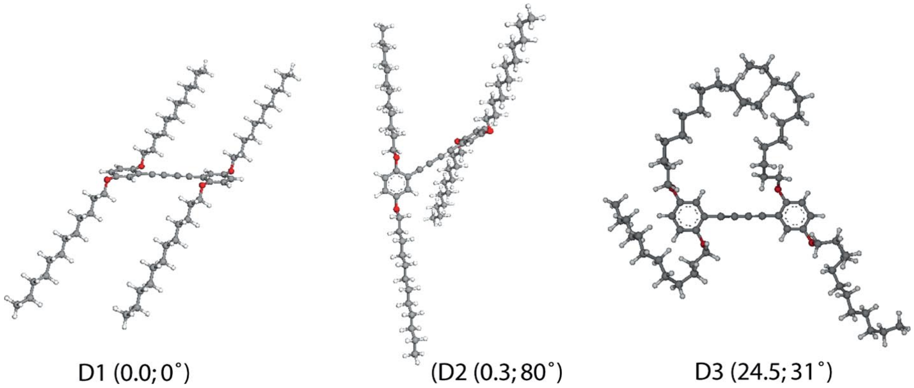

Figure 7. Some representative examples of conformer geometries of dimer **4**. Relative stability (kcal/mol) and the value of the dihedral angles of the phenyl rings are reported in parentheses.

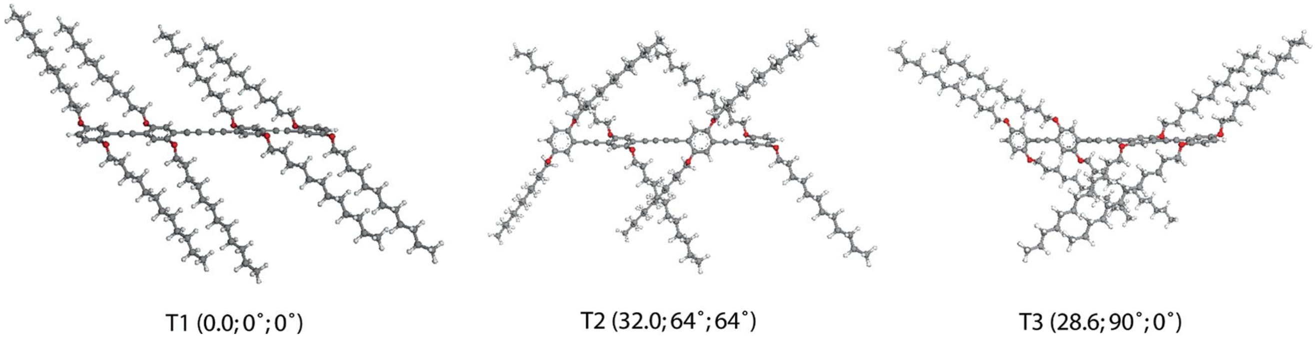

Figure 8. Some representative examples of conformer geometries of tetramer **8**. Relative stability (kcal/mol) and the values of the dihedral angles of the phenyl rings between the internal and external rings are reported in the parentheses.

which the oligomers are embedded (solution, solid state). In contrast, for tetramer **8** (Figure 8), an energy difference of 32 kcal/mol is found between the conformer with dihedral angles of the phenyl rings equal to 0° (T1) and 64° (T2), respectively. In this case, there are more significant alignment effects on the aliphatic chains with respect to the dimer because the "external" phenyl rings are spaced by a single triple bond, which reduces their randomization. These results imply that for dimer **4**, at room temperature, almost all the conformational isomers are present with a comparable population weight, whereas for tetramer **8** the dominant conformations should be those with all the phenyl rings lying on the same plane (see T1 in Figure 8). On the basis of this analysis, we refined the structure of D1, D2, T1 and T2 at the B3LYP/6-311G** level. With respect to the molecular mechanics (MM/UFF) results, the dihedral angle between the phenyl rings increases from 0° to 18° for D1, decreases from 80° to 53° for D2, and does not change for T1, whereas for T2 it decreases to 44° from 64°. Finally, as expected, for the oligomer backbones, the ab initio calculated bond length of the triple bonds becomes more relaxed 1.210–1.220 Å (vs. 1.200–1.205 Å of MM/UFF) and those of the single bonds more compressed 1.350–1.360 Å (vs. 1.411–1.415 Å of MM/UFF) as a consequence of a better description, with the ab initio calculations of the conjugation effects on these oligomers, which plays an important role in the description of the electronic transitions.

The results of the time dependence (TD) calculations are summarized in Table 2.

Table 2. Calculated (TD-B3LYP/6-311G**) wavelength (nm) and oscillator strengths for the first optical allowed (S) and triplet (T) excited state and their energy difference ΔE_{S-T} (cm^{-1}), for the model systems.

Structure[a]	S [nm]	Oscillator strength	T [nm]	ΔE_{S-T} [cm^{-1}]
D1	376.1	1.147	412.1	2307
D2	351.1	0.830	351.4	24
T1	459.8	2.959	504.7	1936
T2	404.1	2.037	412.4	500

[a] ab initio geometry.

Comparison between Table 1 and Table 2 reveals good agreement with the experimental results: (1) for dimer **4**, the main absorption peak is experimentally observed at 350 nm and calculated to be 351 nm for D2; for tetramer **8** at 400 nm (calculated 404 nm for T2). (2) Because the singlet and triplet excited states for the conformer D2 have practically the same energy, a high probability of intersystem crossing between these states could occur, with the consequence of a luminescence quenching, as experimentally observed. On the other hand, the energy gap between the singlet and triplet excited state for tetramer **8** is greater. Consequently, this quenching channel is unfavourable and the

Table 3. Two-photon spectroscopy data for pPEOC12-Dac in $CHCl_3$.

pPEOC12-Dac	N_π[a]	ν_{io} [cm^{-1}][b]	ν_{f0} [cm^{-1}][c]	Γ [cm^{-1}][d]	σ_2 [GM][e]	S [GMcm^{-1}][f]
Dimer **4**	32	28600	29850	2050	8	1.38×10^4
Tetramer **8**	64	25000	29400	2050	360	3.62×10^5
Hexamer **12**	96	23500	28600	2050	2100	1.80×10^6
Octamer **15**	128	23000	26700	2050	5000	5.37×10^6

[a] Number of π electrons per oligomer. [b] 1PA-allowed transition frequency. [c] 2PA-allowed transition frequency. [d] 2PA bandwidth. [e] 2PA cross-section. [f] Conjugation signature.

oligomer (and those with a greater number of repeat phenylenethynylene units) should be fluorescent, as experimentally observed.

Two-Photon Absorption

Two-photon absorption (2PA) is a nonlinear optical process that can be used in fluorescence microscopy, optical data storage, nonlinear optics and microfabrication.[16] Due to the large fluorescence quantum yield obtained for the oligomer series, 2PA spectroscopy was carried out in chloroform (Figure 9) using the fluorescence technique.[17] The data are summarized in Table 3.

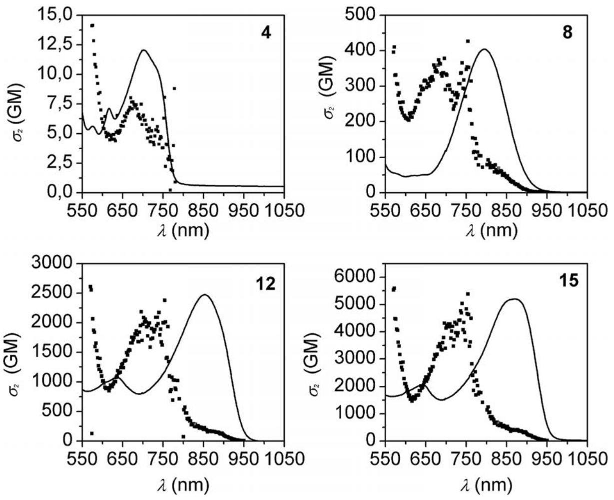

Figure 9. Two-photon spectra in $CHCl_3$ for the pPEOC12-Dac series. The 1PA spectrum shifted by 2λ is also shown.

All the spectra show a rather weak peak or shoulder coincident with the S0→S1 transition. This result indicates that the centre of symmetry is broken sufficiently to give a slight permanent dipole moment. A much stronger transition just above the S0→S1 band is likely a g-g transition that is forbidden in the corresponding 1PA. The 2PA features shift to the red with increasing chain length in a similar way to the 1PA spectrum shift.

The spectra behave according to a three-level model, so we calculated the conjugation signature S:[18]

$$S = \sigma_2^m \Gamma_f \left(2\frac{\nu_{io}}{\nu_{fo}} - 1\right)^2 = C|\mu_{01}|^2|\mu_{if}|^2$$

where σ_2^m is the 2PA cross-section, Γ_f is the 2PA bandwidth (cm^{-1}), ν_{io} is the energy of the 1PA transition (cm^{-1}), and ν_{fo} is the energy of the 2PA transition (cm^{-1}). The quantity C is a constant, μ_{01} is the transition dipole moment of the 1PA transition and μ_{if} is the transition dipole moment between the 1PA and 2PA transitions. A fit to a power law gives:

$$S = AN_\pi^k$$

where N_π is the number of π electrons in the oligomer. The dependence of S on N_π reveals the extent of conjugation. When there is strong conjugation through the oligomer, $\mu \approx N_\pi$, giving $S \approx N_\pi^4$. When $k < 4$, the excited states are more localized. A plot of S vs. N_π (the number of π electrons in the oligomer) is presented in Figure 10. The value of k is calculated to be 4.3, suggesting strong conjugation to the oligomers resulting from a rod-like shape. Hexamer **12** and, particularly, octamer **15** present quite large cross sections in the red region (between 650 and 750 nm).

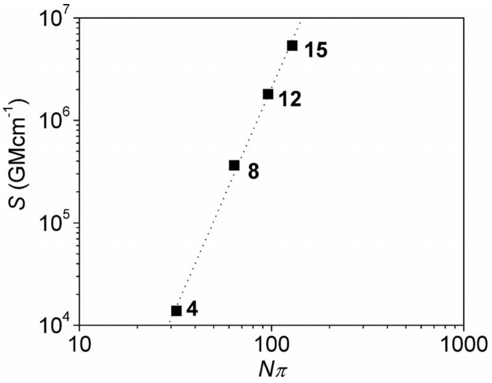

Figure 10. Plot of conjugation signature S vs. the number of π electrons in the pPEOC12-Dac series (N).

Conclusions

A facile route by Sonogashira reaction is reported for the synthesis of 2,5-bis(dodecanoxy)phenyleneethynylene-butadiynes having 2, 4, 6 and 8 phenyl rings. The electron-donor character of the dodecanoxy chains favour acetylene-acetylene coupling, which proceed in quantitative yields, whereas the yields are rather modest for the cross-coupling between iodo or bromo aryl acetylenes. The molecular structure of the series was corroborated by ^1H, ^{13}C, DEPT-135, and APT ^{13}C NMR studies and by FTIR and FT-Raman spectroscopy. The optical properties in solution were observed to be very similar to those of the corresponding phenyleneethynylene moieties with the exception of the dimer, in which intersystem crossing is more favoured due to the low energy gap between the singlet and triplet states as revealed by theoretical calculations. The hexamer and octamer, in particular, show a large quantum yield of 0.78 and 0.82, respectively, and 2PA cross-sections of 10^3 GM, which make them good candidates for multiphoton microscopy applications.

Experimental Section

Materials: The following materials were obtained from Aldrich and used without further purification: hydroquinone, 1-bromododecane, copper(I) iodide, dichlorobis(triphenylphosphane)palladium(II), tetrabutylammonium fluoride (TBAF; 1.0 M in THF), trimethylsilyl acetylene (TMSA) and NaH. CH_2Cl_2, $CHCl_3$, methanol, hexanes and toluene were purchased from Aldrich and Baker. THF and triethylamine (Et_3N) were distilled from KOH, and THF then from sodium/benzophenone complex. Solvents used for the optical characterization were spectroscopic grade from Aldrich.

Molecular Characterization: ^1H and ^{13}C NMR spectroscopic data were obtained at room temperature with a JEOL (300 MHz) or a BRUKER AVANCE III (500 MHz) spectrometer using $CDCl_3$ as solvent and internal reference. MALDI-TOF-MS was carried out with a Waters/Micromass MALDI micro MX mass spectrometer operated in reflection mode using α-cyano-4-hydroxycinnamic acid as a matrix. Raman scattering spectra were obtained on powders with an 830 nm diode Laser and a Renishaw system. Infrared spectra were obtained with a Nicolet Magna 550 spectrophotometer (FTIR) on KBr crystals.

UV/Vis absorption spectra were measured with a Shimadzu 2401PC spectrophotometer. The emission spectra were recorded with a Perkin–Elmer LS 50B spectrofluorimeter by exciting at 10 nm below the lower energy peak. Fluorescence quantum yields in solution (ϕ_F) were determined by using a reported procedure[19] and using quinine sulfate (0.1 M in H_2SO_4; $\phi = 0.54$ at 347 nm) as standard. The experiments were conducted by controlling the temperature at 25.0 ± 0.5 °C with a water circulating bath. Four solutions with absorbance of lower than 0.1 at the excitation wavelength were analyzed for each sample. Fluorescence lifetimes were obtained at room temperature by the TCSPC technique with a Horiba Jobin Yvon TemPro instrument with nanoLED excitation at 370 nm for tetramer **8**, hexamer **12** and octamer **15**. For dimer **4**, a nanoLED of 295 nm was used because this oligomer emits near 370 nm. Fits were performed with DAS6 software available in the instrument. Two-photon (2PA) spectra were measured at ambient conditions according to published methods.[20]

Theoretical Studies: Theoretical simulations were carried out on dimer **4** and tetramer **8**, using the Gaussian 09 software.[21] To reduce the computational time required, we investigated the phenyl ring torsional barriers of the two model systems in the framework of the molecular mechanics approach using the UFF force field.[22] The geometry of the most stable conformers was then further optimized at the B3LYP/6-311G** level. Electronic transitions were computed by using the TD-B3LYP/6-311G** approach and taking into account solvent effects with the polarizable continuum model (PCM). Moreover, because the aliphatic tails should not make a significant contribution to the electronic nature of the excitations (at least for the lowest levels) they were replaced by a $-OCH_3$ group.[23]

General Procedure for the Cross-Coupling of an Acetylene with Bromo or Iodo Aryls: To a two-necked round-bottomed flask containing $[(Ph_3P)_2PdCl_2]$ (2.5 mol-%), CuI (1.5 mol-%) and the aryl halide was added dry and degassed 95:5 (v/v) Et_3N/THF by using a cannula. The mixture was heated at 60 °C for 5 min (by Goldt's method, it was cooled to ca. 0 °C). The acetylene monomer dissolved in degassed Et_3N was then added by using a syringe and the mixture was stirred vigorously for 16 h at 60 °C (by the Goldt method after adding the acetylene, the reaction was left to reach the room temperature and stirred for 48 h). The mixture was filtered to remove the ammonium salt and the organic phase was ready for the next purification process.

General Procedure for the Homocoupling of an Acetylene: To a two-necked round-bottomed flask containing $[(Ph_3P)_2PdCl_2]$ (2.5 mol-%), CuI (3.0 mol-%) and the acetylene compound was added dry and degassed 95:5 (v/v) Et_3N/THF by using a cannula. The reaction was then heated to 80 °C and stirred under nitrogen overnight. The mixture was filtered to eliminate the ammonium salt and the organic phase was ready for the next purification process.

General Procedure for Trimethylsilyl (TMS) Cleavage: A round-bottomed flask was charged with the (trimethylsilyl)ethynyl compound, THF, and two drops of water and stirred until total dissolution of the compound. TBAF was added (0.2 equiv. per silyl group, 1 M solution in THF) and the mixture was stirred at room temperature for 30 min. The reaction was stopped by passing it thought a plug of silica gel. After THF evaporation, the product was dried in vacuo for 2 h and then used without further purification.

Compounds 1–3, 5 and 6: Synthesized as reported in Ref.[8]

1,4-Bis{[2,5-bis(dodecanoxy)phenyl]buta-1,3-diyne} (4): Applying the procedure for the homocoupling of acetylenes: In a flask containing $[(Ph_3P)_2PdCl_2]$ (18.63 mg, 0.02655 mmol), CuI (6.07 mg, 0.032 mmol) and **1** (500 mg, 1.06 mmol) was added by using a cannula triethylamine (80 mL) and THF (8 mL). The mixture was heated at 80 °C for 16 h. After filtering the ammonium salt and removal of the solvent, the crude product was first precipitated in methanol, purified by column chromatography (SiO_2; hexanes–CH_2Cl_2, 1:1; $R_f = 0.7$) and then by preparative gel permeation chromatography column (Biorad; Bio-Beads SX1, toluene) to afford, after solvent evaporation, **4** (95% yield) as a white powder; m.p. 83–87 °C. ^1H NMR (300 MHz, $CDCl_3$): $\delta = 6.98$ (d, $J = 2.7$ Hz, 2 H, Ar-$H_{o\text{-ynes}}$), 6.83 (dd, $J_1 = 9.0$, $J_2 = 2.7$ Hz, 2 H, Ar-H_{ext}), 6.78 (d, $J = 9.0$ Hz, 2 H, Ar-H_{ext}), 3.97, 3.87 (2 × t, $J = 6.6$ Hz, 8 H, CH_2-α-O), 1.76 (m, 8 H, CH_2-β-O), 1.45 (m, 8 H, CH_2-γ-O), 1.26 (br. s, 64 H, CH_2), 0.87 (br. m, 2 H, CH_3) ppm. ^{13}C NMR (75 MHz, $CDCl_3$): $\delta = 14.22$ (CH_3), 22.80 (CH_2), 26.09 (C-γ-O), 29.36 (C-β-O), 29.48 (CH_2), 29.75 (CH_2), 32.01 (CH_2), 68.78 and 70.01 (C-α-O), 77.91, 78.76 (C≡C), 112.49, 114.17, 115.48, 117.66, 119.18 (Ar), 152.78, 153.39, 155.53 (Ar*C*-O) ppm. UV/Vis ($CHCl_3$): λ_{max} (ε, $M^{-1}\,cm^{-1}$) = 350 nm (1.68×10^4). MALDI-TOF: *m/z* calcd. for $C_{64}H_{106}O_4$ $[M]^{\cdot+}$ 938.8; found 938.6.

Dodecanoxy Mono Bromine Terminated Trimer 7: Applying the procedure used for the cross-coupling of a bromo aryl with an acetylene: In a flask containing $[(Ph_3P)_2PdCl_2]$ (7.25 mg, 0.0103 mmol), CuI (1.96 mg, 0.0103 mmol) and **6** (324 mg, 0.345 mmol) was added Et_3N (100 mL) and THF (10 mL) under nitrogen. The mixture was heated at 50 °C for 15 min and then cooled to 0 °C. Compound **2** (224.48 mg, 0.345 mmol) in anhydrous and degassed Et_3N (5 mL) was added by using a syringe. The mixture was allowed to reach room temperature and stirred for 48 h. After filtering the ammonium salt and evaporating the solvent, the crude product was purified first by precipitation in methanol, then by silica gel chromatography (hexanes–$CHCl_3$, 2:1; R_f = 0.4) and finally passed through a preparative gel permeation chromatography column (Biorad; Bio-Beads SX1, toluene) to afford, after solvent evaporation, **7** (59% yield) as a yellow powder; m.p. 76–80 °C. ^{1}H NMR (500 MHz, $CDCl_3$): δ = 7.09 (s, 1 H, Ar-H), 7.02–6.99 (m, 4 H, Ar-H), 6.81 (s, 2 H, Ar-H), 4.04–3.95 (m, 10 H, CH_2-α-O), 3.90 (t, J = 6.4 Hz, 2 H, CH_2-α-O), 1.98–1.70 (m, 12 H, CH_2-β-O), 1.49–1.38 (m, 12 H, CH_2-γ-O), 1.38–1.15 (br. s, 108 H, -CH_2-; theoretical value 96 H), 0.90–0.76 (br. m, 20 H, CH_3; theoretical value 18 H) ppm. ^{13}C NMR (125.6 MHz, $CDCl_3$): δ = 14.15 (CH_3), 22.74 (CH_2), 25.99–26.07 (C-γ-O), 29.31 (C-β-O), 29.42–29.55 (CH_2), 29.72–31.98 (CH_2), 68.74–69.83 (C-α-O), 89.86, 90.74, 90.76, 91.66 (-C≡C-), 113.16, 113.26, 114.04, 114.08, 114.46, 114.75, 116.64, 117.43, 117.80, 118.35, 118.62 (Ar), 149.56, 152.95, 153.57, 154.07, 154.10 (Ar*C*-O) ppm. UV/Vis ($CHCl_3$): λ_{max} (ε, $M^{-1}cm^{-1}$) = 381 nm (5.86×10^4).

Compound 8: Applying the procedure for the homocoupling of acetylenes: In a flask containing $[(Ph_3P)_2PdCl_2]$ (6 mg, 8.0×10^{-3} mmol), CuI (2 mg (8.0×10^{-3} mmol) and **6** (250 mg, 0.142 mmol) was added by using a cannula Et_3N (40 mL) and THF (4 mL). The mixture was heated at 80 °C for 16 h. After filtering the ammonium salt and evaporation of the solvent, the crude product was precipitated in methanol, purified by column chromatography (SiO_2; hexanes–CH_2Cl_2, 2:1; R_f = 0.3) and then by preparative gel permeation chromatography (Biorad; Bio-Beads SX1, toluene) to afford, after solvent evaporation, **8** (93% yield) as a yellow powder; m.p. 83–85 °C. ^{1}H NMR (300 MHz, $CDCl_3$): δ = 7.00, 6.97 (2× s, 6 H, Ar-$H_{o\text{-ynes}}$), 6.81 (s, 4 H, Ar-H_{ext}), 3.98, 3.89 (2× t, J = 3 Hz, 16 H, CH_2-α-O), 1.81 (br. m, 16 H, CH_2-β-O), 1.47 (br. m, 16 H, CH_2-γ-O), 1.23 (br. s, 128 H, CH_2), 0.87 (br. m, 24 H, CH_3) ppm. ^{13}C NMR (75 MHz, $CDCl_3$): δ = 14.19 (CH_3), 22.78 (CH_2), 26.09 (C-γ-O), 29.36 (C-β-O), 29.46 (CH_2), 29.75 (CH_2), 32.01 (CH_2), 68.76, 69.82 and 70.05 (C-α-O), 79.30, 79.64 (DacC≡C), 89.73, 92.32 (ynesC≡C), 112.40, 113.91, 114.42, 115.80, 116.82, 117.19, 118.05, 118.62 (Ar), 152.94, 153.39, 154.13, 155.06 (Ar*C*-O). UV/Vis ($CHCl_3$): λ_{max} (ε, $M^{-1}cm^{-1}$) = 400 nm (7.39×10^4). MALDI-TOF: *m*/*z* calcd. for $C_{128}H_{210}O_8$ $[M]^{\cdot+}$ 1875.6; found 1875.7.

Compound 9: Applying the procedure for the cross-coupling of a bromo aryl with an acetylene: In a flask containing $[(Ph_3P)_2PdCl_2]$ (4.2 mg, 0.006 mmol), CuI (1.5 mg, 0.0072 mmol) and **7** (350 mg, 0.239 mmol) was added triethylamine (50 mL) and THF (5 mL) under nitrogen. The mixture was heated at 50 °C for 15 min, then TMSA (0.12 mL, 0.72 mmol) was added by using a syringe. The mixture was stirred and heated overnight at 80 °C. After filtering off the ammonium salt and evaporating the solvent, the crude product was purified by chromatography (SiO_2; hexanes–CH_2Cl_2, 2:1; R_f = 0.4) to give, after solvent evaporation, **9** (63% yield) as a yellow powder; m.p. 64–71 °C. ^{1}H NMR (300 MHz, $CDCl_3$): δ = 7.03–6.92 (br. s, 5 H, Ar-H), 6.81 (br. s, 2 H, Ar-H), 4.06–3.93 (m, 12 H, CH_2-α-O), 3.89 (t, J = 6.4 Hz, 2 H, CH_2-α-O), 1.90–1.70 (m, 12 H, CH_2-β-O), 1.56–1.42 (m, 12 H, CH_2-γ-O), 1.40–1.15 (br. s, 114 H, CH_2-; theoretical value is 96 H), 0.92–0.83 (br. m, 19 H, CH_3; theoretical value is 18 H), 0.26 (s, 7.5 H, $SiMe_3$; theoretical value is 9 H) ppm. ^{13}C NMR (75.4 MHz, $CDCl_3$): δ = 0.06 ($SiMe_3$), 14.20 (CH_3), 22.78 (CH_2), 25.69–26.14 (CH_2-γ-O), 29.46 (CH_2-β-O), 29.52–29.58 (CH_2), 29.60–29.80 (CH_2), 32.02 (CH_2), 68.06, 68.75, 69.51, 69.77, 70.02 (CH_2-α-O), 89.90, 90.77, 91.33, 91.71, 100.09, 101.32 (-C≡C-), 113.68, 114.08, 114.45, 114.75, 116.66, 117.08, 117.41, 117.55, 118.62 (Ar), 152.95, 153.40, 153.56, 154.08, 154.27 (Ar*C*-O) ppm. UV/Vis ($CHCl_3$): λ_{max} (ε, M^{-1} cm^{-1}) = 389 nm (3.90×10^4).

Compound 11: Applying the procedure for the cross-coupling of a bromo aryl with an acetylene: In a flask containing $[(Ph_3P)_2PdCl_2]$ (17 mg, 0.230 mmol), CuI (3 mg, 0.014 mmol) and **2** (601 mg, 0.923 mmol) was added triethylamine (100 mL) and THF (10 mL) under nitrogen. The mixture was heated at 50 °C for 15 min, then **10** (1300 mg, 0.923 mmol) in dry and degassed Et_3N (5 mL) was added by using a cannula. The mixture was allowed to react at 80 °C for 16 h. After filtering the ammonium salt and evaporation of the solvent, the crude product was purified first by precipitation in methanol, then by silica gel chromatography (hexanes–$CHCl_3$, 1:1; R_f = 0.4) and finally by preparative gel permeation chromatography (Biorad; Bio-Beads SX1, toluene) to afford, after solvent evaporation, **11** (46% yield) as a yellow powder; m.p. 84–87 °C. ^{1}H NMR (500 MHz, $CDCl_3$): δ = 7.09 (br. s, 1 H, Ar-H), 7.02–6.98 (br. s, 6 H, Ar-H), 6.81(br. s, 2 H, Ar-H), 4.05–3.94 (m, 14 H, CH_2-α-O), 3.90 (t, J = 6.3 Hz, 2 H, CH_2-α-O), 1.90–1.70 (m, 16 H, CH_2-β-O), 1.55–1.42 (m, 16 H, CH_2-γ-O), 1.41–1.18 (br. s, 136 H, CH_2-; theoretical value is 128 H), 0.92–0.84 (br. m, 26 H, CH_3; theoretical value is 24 H) ppm. ^{13}C NMR (125.6 MHz, $CDCl_3$): δ = 14.20 (CH_3), 22.78 (CH_2), 25.95–26.12 (CH_2-γ-O), 29.35 (CH_2-β-O), 29.55–29.80 (CH_2), 32.02 (CH_2), 68.76, 69.76, 70.03, 70.08, 70.16 (CH_2-α-O), 89.93, 90.76, 90.93, 91.45, 91.74 (-C≡C-), 113.13, 113.33, 114.15, 114.26, 114.46, 114.55, 114.76, 116.66, 117.38, 117.45, 117.81, 118.35, 118.65 (Ar), 149.58, 152.97, 153.60, 154.12 (Ar*C*-O) ppm. UV/Vis ($CHCl_3$): λ_{max} (ε, $M^{-1}cm^{-1}$) = 400 nm (6.87×10^4).

Compound 12: Applying the procedure for the homocoupling of acetylenes: In a flask containing $[(Ph_3P)_2PdCl_2]$ (3 mg, 0.0036 mmol), CuI (1 mg, 0.004 mmol) and **10** (200 mg, 0.142 mmol) was added by using a cannula Et_3N (25 mL) and THF (2.5 mL). The mixture was heated at 80 °C for 16 h. After filtering the ammonium salt and evaporation of the solvent, the crude product was first precipitated in methanol, then purified by column chromatography (SiO_2; hexanes–CH_2Cl_2, 1.5:1; R_f = 0.4) and finally passed through a preparative gel permeation chromatography column (Biorad; Bio-Beads SX1, toluene) to afford, after solvent evaporation, **12** (87% yield) as a yellow powder; m.p. 108–112 °C. ^{1}H NMR (300 MHz, $CDCl_3$): δ = 7.01, 7.0, 6.99, 6.98 (4× s, 10 H, Ar-$H_{o\text{-ynes}}$), 6.81 (s, 4 H, Ar-H_{ext}), 3.99, 3.90 (2× t, J = 6.3 Hz, 24 H, CH_2-α-O), 1.82 (br. m, 24 H, CH_2-β-O), 1.46 (br. m, 24 H, CH_2-γ-O), 1.23 (br. s, 192 H, CH_2), 0.86 (br. m, 36 H, CH_3) ppm. ^{13}C NMR (75 MHz, $CDCl_3$): δ = 14.18 (CH_3), 22.77 (CH_2), 26.09 (C-γ-O), 29.26 (C-β-O), 29.45 (CH_2), 29.75 (CH_2), 32.01 (CH_2), 68.77, 69.82 and 70.04 (C-α-O), 79.42, 79.69 (DacC≡C), 89.89, 91.28, 91.78, 92.38 (ynesC≡C), 112.60, 113.97, 114.09, 114.48, 114.92, 115.63, 116.71, 117.16, 117.26, 117.45, 118.01, 118.64 (Ar), 152.96, 153.40, 153.57, 153.66, 154.10, 155.08 (Ar*C*-O) ppm. UV/Vis ($CHCl_3$): λ_{max} (ε, $M^{-1}cm^{-1}$) = 425 nm (11.6×10^4). MALDI-TOF: *m*/*z* calcd. for $C_{192}H_{314}O_{12}$ $[M]^{\cdot+}$ 2812.4; found 2812.4.

Compound 13: Applying the procedure for the cross-coupling of a bromo aryl with an acetylene: In a flask containing $[(Ph_3P)_2PdCl_2]$ (4 mg, 6.2114×10^{-3} mmol), CuI (ca. 1 mg, 3.1057×10^{-3} mmol) and **11** (400 mg, 0.207 mmol), was added triethylamine (70 mL) and THF (7 mL) under nitrogen. The mixture was heated at 50 °C for 15 min, then TMSA (0.10 mL, 0.621 mmol) was added by using a syringe. The mixture was stirred and heated overnight at 80 °C. After filtering off the ammonium salt and evaporating the solvent, the crude product was purified by chromatography (SiO_2; hexanes/CH_2Cl_2, 1:1; R_f = 0.4) to give, after solvent evaporation, **13** (52% yield) as a yellow powder; m.p. 73–77 °C. ^{1}H NMR (500 MHz, $CDCl_3$): δ = 7.04–6.98 (br. s, 5 H, Ar-H), 6.96 (br. s, 1 H, Ar-H), 6.95 (br. s, 1 H, Ar-H), 6.83 (br. s, 2 H, Ar-H), 4.06–3.96 (m, 14 H, CH_2-α-O), 3.92 (t, J = 6.4 Hz, 2 H, CH_2-α-O), 1.90–1.73 (m, 16 H,

CH_2-β-O), 1.56–1.42 (m, 16 H, CH_2-γ-O), 1.41–1.21 (br. s, 142 H, CH_2-; theoretical value is 128 H), 0.92–0.84 (br. m, 26 H, CH_3; theoretical value is 24 H), 0.28 (s, 7 H, $SiMe_3$; theoretical value is 9 H) ppm. ^{13}C NMR (125.6 MHz, $CDCl_3$): δ = –0.02 ($SiMe_3$), 14.10 (CH_3), 22.69 (CH_2), 25.94–26.12 (CH_2-γ-O), 29.38 (CH_2-β-O), 29.44–29.54 (CH_2), 29.55–29.80 (CH_2), 31.93 (CH_2), 68.70, 69.47, 69.60–69.80, 69.98 (CH_2-α-O), 89.85, 91.40, 91.61, 91.68, 100.03, 101.26 (-C≡C-), 113.71, 114.08, 114.12, 114.24, 114.44, 114.49, 114.69, 116.59, 117.08, 117.35, 117.41, 117.54, 118.58 (Ar), 152.90, 153.37, 153.53, 154.07, 154.03, 154.23 (Ar*C*-O) ppm. UV/Vis ($CHCl_3$): λ_{max} (ε, $M^{-1}cm^{-1}$) = 405 nm (10.217×10^4).

Compound 15: Applying the procedure used for the homocoupling of acetylenes: In a flask containing [$(Ph_3P)_2PdCl_2$] (2.0 mg, 0.0026 mmol), CuI (ca. 1.0 mg, 0.0031 mmol) and **14** (193 mg, 0.10271 mmol) was added by using a cannula, Et_3N (25 mL) and THF (2.5 mL). The mixture was heated at 80 °C for 16 h. After filtering the ammonium salt and evaporation of the solvent, the crude product was precipitated in methanol, purified by column chromatography (SiO_2; hexanes/CH_2Cl_2, 1.5:1; R_f = 0.3) and then by preparative gel permeation chromatography (Biorad; Bio-Beads SX1, toluene) to afford, after solvent evaporation, **15** (89% yield) as a yellow powder; m.p. 124–127 °C. ^1H NMR (300 MHz, $CDCl_3$): δ = 7.01–6.98 (4× br. s, 14 H, Ar-$H_{o\text{-ynes}}$), 6.81 (s, 4 H, Ar-H_{ext}), 4.02 (br. s, 16 H, CH_2-α-O), 3.90 (t, *J* = 6.3 Hz, 16 H, CH_2-α-O), 1.83 (br. m, 32 H, CH_2-β-O), 1.50 (br. m, 32 H, CH_2-γ-O), 1.24 (br. s, 256 H, CH_2), 0.86 (br. m, 48 H, CH_3) ppm. ^{13}C NMR (75 MHz, $CDCl_3$): δ = 14.17 (CH_3), 22.76 (CH_2), 26.11 (C-γ-O), 29.27 (C-β-O), 29.46 (CH_2), 29.76 (CH_2), 32.01 (CH_2), 68.78, 69.82 and 70.05 (C-α-O), 79.44, 79.70 (DacC≡C), 89.92, 91.44, 91.70, 91.83, 92.36 (ynesC≡C), 112.64, 114.15, 114.50, 114.72, 114.79, 115.61, 116.67, 117.18, 117.46, 118.02, 118.65 (Ar), 152.97, 153.43, 153.60, 153.67, 154.10, 155.09 (Ar*C*-O). UV/Vis ($CHCl_3$): λ_{max} (ε, $M^{-1}cm^{-1}$) = 435 nm (16.99×10^4). MALDI-TOF: *m/z* calcd. for $C_{256}H_{418}O_{16}$ $[M]^{\cdot+}$ 3749.2; found 3748.8.

Supporting Information (see footnote on the first page of this article): DEPT-135, APT, ^{13}C NMR spectra for the oligomers in $CDCl_3$; MALDI-TOF MS; Additional absorption and fluorescence spectra of tetramer **8** and TCSPC data for dimer **4**, hexamer **12** and octamer **15** in chloroform.

Acknowledgments

The authors wish to acknowledge the Mexican National Council for Science and Technology (CONACYT) for financial support through project 98513R and the United States Air Force Office for Scientific Research (AFOSR) through grant FA9550-10-1-0173.

---

[1] See for instance the following recent reviews and references cited therein: a) U. H. F. Bunz, in: *Conjugated Polymers. Theory, Synthesis Properties and Characterization* (Eds.: T. A. Skotheim, J. R. Reynolds), CRC Press, Boca Raton, **2007**, chapter 6, p. 1–51; b) I. Moggio, E. Arias, in: *Biomimetic and Supramolecular Systems Research* (Ed.: A. H. Lima), Nova Science Publishers Inc., New York, **2008**, chapter VIII, p. 179–212; c) *Advances in Polymer Science* (Ed.: C. Weder), Springer, Berlin, **2005**, vol. 177; d) S. W. Thomas, G. D. Joly, T. M. Swager, *Chem. Rev.* **2007**, *107*, 1339–1386.

[2] a) A. Khatyr, R. Ziessel, *J. Org. Chem.* **2000**, *65*, 3126–3134; b) A. Godt, C. Franzan, S. Veit, V. Enkelmann, M. Pannier, G. J. Jeschke, *J. Org. Chem.* **2000**, *65*, 7575–7582; c) M. Wielopolski, C. Atienza, T. Clark, D. M. Guidi, N. Martin, *Chem. Eur. J.* **2008**, *14*, 6379–6390; d) C. Wang, A. S. Batsanov, M. R. Bryce, *J. Org. Chem.* **2006**, *71*, 108–116.

[3] a) D. Mössinger, S.-S. Jester, E. Sigmund, U. Müller, S. Höger, *Macromolecules* **2009**, *42*, 7974–7978; b) S.-S. Jester, A. Idelson, D. Schmitz, F. Eberhagen, S. Höger, *Langmuir* **2011**, *27*, 8205–8215; c) P. Zalake, K. G. Thomas, *Langmuir* **2013**, *29*, 2242–2249.

[4] P. Siemsen, R. C. Livingston, F. Diederich, *Angew. Chem.* **2000**, *112*, 2740; *Angew. Chem. Int. Ed.* **2000**, *39*, 2632–2657.

[5] D. A. M. Egbe, E. Birckner, E. Klemm, *J. Polym. Sci., Part A: Polym. Chem.* **2002**, *40*, 2670–2679.

[6] a) H. A. Dieck, R. F. Heck, *J. Organomet. Chem.* **1975**, *93*, 259–263; b) R. F Heck, *Palladium Reagent in Organic Syntheses*, Academic Press, New York, **1990**; c) C. Amatore, A. Jutand, A. Suarez, *J. Am. Chem. Soc.* **1993**, *115*, 9531–9541.

[7] U. Ziener, A. Godt, *J. Org. Chem.* **1997**, *62*, 6137–6143.

[8] G. Castruita, E. Arias, I. Moggio, F. Pérez, D. Medellin, R. Torres, R. Ziolo, A. Olivas, E. Giorgetti, M. Muniz-Miranda, *J. Mol. Struct.* **2009**, *936*, 177–186.

[9] A. M. Hoberg, D. M. Haddleton, P. J. Derrick, A. T. Jackson, J. H. Scrivens, *Eur. Mass Spectrom.* **1998**, *4*, 435–440.

[10] I. Moggio, M. Alloisio, A. Cravino, D. Comoretto, P. Piaggio, G. F. Musso, G. Garbarino, C. Cuniberti, C. Dell'Erba, G. Dellepiane, *J. Chem. Soc. Perkin Trans. 2* **1998**, *2*, 2249–2254.

[11] a) G. Wegner, *Z. Naturforsch. B* **1969**, *24*, 824–831; b) H.-J. Cantow, *Polydiacetylenes*, Springer-Verlag, Berlin, Heidelberg, New York, Tokyo, **1984**.

[12] I. B. Berlman, *Handbook of Fluorescence Spectra of Aromatic Molecules*, 2nd ed., Academic Press, London, New York, **1971**.

[13] a) P. V. James, P. K. Sudeep, C. H. Suresh, K. G. Thomas, *J. Phys. Chem. A* **2006**, *110*, 4329–4337; b) L. T. Liu, D. Yaron, M. I. Sluch, M. A. Berg, *J. Phys. Chem. B* **2006**, *110*, 18844–18452; c) Y. Matsunaga, K. Takeshi, T. Akasaka, A. R. Ramesh, P. V. James, K. G. Thomas, P. V. Kamat, *J. Phys. Chem. B* **2008**, *112*, 14539–14547; d) N. Li, K. Jia, S. Wang, A. Xia, *J. Phys. Chem. A* **2007**, *111*, 9393–9398.

[14] G. Duvanel, J. Grilj, A. Schuwey, A. Gossauerb, E. Vauthey, *Photochem. Photobiol. Sci.* **2007**, *6*, 956–963.

[15] Y. Nagano, T. Ikoma, K. Akiyama, S. J. Tero-Kubota, *Chem. Phys.* **2001**, *114*, 1775–1784.

[16] As a general review on multiphoton absorption spectroscopy, see: G. S. He, L. S. Tan, Q. Zheng, P. N. Prasad, *Chem. Rev.* **2008**, *108*, 1245–1330.

[17] A. Karotki, M. Drobizhev, M. Kruk, C. Spangler, E. Nickel, N. Mamardashvili, A. Rebane, *J. Opt. Soc. Am. B* **2003**, *20*, 321–332.

[18] M. Drobizhev, Y. Stepanenko, A. Rebane, C. J. Wilson, T. E. O. Screen, H. L. Anderson, *J. Am. Chem. Soc.* **2006**, *128*, 12432–12433.

[19] A. T. R. Williams, S. A. Winfield, J. N. Millar, *Analyst* **2003**, *108*, 1067–1071.

[20] a) N. S. Makarov, M. Drobizhev, A. Rebane, *Opt. Express* **2008**, *16*, 4029–4047; b) J. E. Rogers, J. E. Slagle, D. M. Krein, A. R. Burke, B. C. Hall, A. Fratini, D. G. McLean, P. A. Fleitz, T. M. Cooper, M. Drobizhev, N. S. Makarov, A. Rebane, K.-Y. Kim, R. Farley, K. S. Schanze, *Inorg. Chem.* **2007**, *46*, 6483–6494; c) A. Rebane, M. Drobizhev, N. S. Makarov, E. Beuerman, J. E. Haley, M. Krein, A. R. Burke, J. L. Flikkema, T. M. Cooper, *J. Phys. Chem. A* **2011**, *115*, 4255–4262.

[21] M. J. Frisch, G. W. Trucks, H. B. Schlegel, G. E. Scuseria, M. A. Robb, J. R. Cheeseman, G. Scalmani, V. Barone, B. Mennucci, G. A. Petersson, H. Nakatsuji, M. Caricato, X. Li, H. P. Hratchian, A. F. Izmaylov, J. Bloino, G. Zheng, J. L. Sonnenberg, M. Hada, M. Ehara, K. Toyota, R. Fukuda, J. Hasegawa, M. Ishida, T. Nakajima, Y. Honda, O. Kitao, H. Nakai, T. Vreven, J. A. Montgomery Jr, J. E. Peralta, F. Ogliaro, M. Bearpark, J. J. Heyd, E. Brothers, K. N. Kudin, V. N. Staroverov, R. Kobayashi, J. Normand, K. Raghavachari, A. Rendell, J. C. Burant, S. S. Iyengar, J. Tomasi, M. Cossi, N. Rega, J. M.

Millam, M. Klene, J. E. Knox, J. B. Cross, V. Bakken, C. Adamo, J. Jaramillo, R. Gomperts, R. E. Stratmann, O. Yazyev, A. J. Austin, R. Cammi, C. Pomelli, J. W. Ochterski, R. L. Martin, K. Morokuma, V. G. Zakrzewski, G. A. Voth, P. Salvador, J. J. Dannenberg, S. Dapprich, A. D. Daniels, Ö. Farkas, J. B. Foresman, J. V. Ortiz, J. Cioslowski, D. J. Fox, *Gaussian 09*, revision B.1, Gaussian, Inc., Wallingford CT, **2009**.

[22] A. K. Rappé, C. J. Casewit, K. S. Colwell, W. M. J. Skiff, *J. Am. Chem. Soc.* **1992**, *114*, 10024–10039.

[23] a) N. Li, A. Wang, A. Xia, *J. Phys. Chem. A* **2007**, *111*, 4329–4336; b) J.-S. K. Yu, W.-C. Chen, C.-H. Yu, *J. Phys. Chem. A* **2003**, *107*, 4268–4275.

Received: February 12, 2013